

A proposal submitted by Dartmouth College to the NASA Living With a Star Targeted Research and Technology Program (Announcement Number NNH06ZDA001N-LWS)

Effects of Stormtime Plasma Redistribution on Magnetosphere-Ionosphere Coupling

PROJECT SUMMARY

The Coupled Magnetosphere-Ionosphere-Thermosphere (CMIT) global simulation model will be used to determine how stormtime ionospheric outflows influence 1) the convective transport of ionospheric plasma at auroral and polar latitudes, 2) the distribution and intensity of field-aligned currents at the ionosphere, and 3) the distribution and dynamics of the ionospheric conductivity and Joule dissipation. CMIT integrates the Lyon-Fedder-Mobarry (LFM) global magnetospheric model with the NCAR Thermosphere-Ionosphere Nested Grid (TING) model. This project takes an important step in modeling the magnetospheric and ionospheric-thermospheric regions as a single connected system by including both electrodynamic and inertial couplings between the regions. To this end, we will utilize and advance a recently implemented, multifluid version of the LFM component of CMIT. Proposed extensions to the CMIT model also include causally driven cusp-region, auroral/polar-cap boundary-region, and polar-wind outflows at LFM's ionospheric boundary, regulated by TING's dynamic specification of the ionosphere. This investigation is directly aligned with the goals of LWS TR&T Focused Science Topic b) Effects of Ionospheric-Magnetospheric Plasma Redistribution on Storms. The results will provide a useful touchstone for interpreting measurements, especially mass composition measurements, from existing NASA satellite missions such as Polar and Cluster, and it anticipates future needs to interpret distributed measurements of ionospheric and magnetospheric dynamics from the imminent THEMIS and TWINS missions, the LWS Radiation Belt and IT Storm Probes, and the GEC and MMS satellites.

Program Element: LWS TR&T Focused Science Topic B. Effects of Ionospheric-Magnetospheric Plasma Redistribution on Storms

Principal Investigator: William Lotko (Dartmouth College)

Co-Investigator: Michael Wiltberger (NCAR/HAO)

Collaborators: John Lyon (Boston University/Dartmouth), Wenbin Wang (NCAR/HAO)

Date: August 31, 2007

Short title: Stormtime Magnetosphere-Ionosphere Coupling

Effects of Stormtime Plasma Redistribution on Magnetosphere-Ionosphere Coupling

Dartmouth College
National Center for Atmospheric Research

Table of Contents

NASA Cover Pages.....	
Project Summary.....	i

Scientific and Technical Management Description

1 Project Overview.....	1
1.1 Objectives, Need and Significance	1
1.2 Technical Approach and Methodology.....	1
1.3 Scientific Impact	2
1.4 Relevance to NASA Programs.....	3
2 Science Issues.....	3
2.1 Ionospheric Convective Transport.....	3
2.2 Magnetospheric Impacts of Outflows.....	4
2.3 Inertial and Electrodynamic Coupling.....	5
3 Modeling Outflows in MI Coupling	6
3.1 Auroral- and Cusp-Region Outflows.....	6
3.2 Polar Outflows and Inflows	9
3.3 Other Outflows.....	10
4 Global Models	11
4.1 LFM Global Magnetospheric Model	11
4.2 TING Model.....	13
4.3 CMIT Model and Outflow Extension.....	13
5 Personnel, Institutional Support, Work Plan and Milestones.....	14
6 Team Coordinator Proposal.....	16
References.....	17
Facilities and Equipment.....	A1
Budget Justification	A2
<i>Detailed Organization Budgets submitted separately via NSPIRES</i>	
Biographical Sketches.....	A8
Current and Pending Support.....	A11
Statements of Commitment.....	A13

1 Project Overview

1.1 Objectives, Need and Significance

The research proposed here takes a major step in advancing our capability to numerically model and analyze the effects of ionospheric outflows on the global geospace environment, in particular the effects of outflows on the stormtime interaction between the magnetosphere and ionosphere. The proposed advances will also apply to the moderately disturbed and relatively quiescent coupled system.

The research investigation will address three primary science questions: How do stormtime ionospheric outflows influence: 1) the convective transport of ionospheric plasma? 2) the distribution and intensity of field-aligned currents at the ionosphere? and 3) the conductivity of the ionosphere and Joule dissipation? We also anticipate new and potentially interesting results on the solar-wind regulation of outflows and on the influences of heavy ion outflows on magnetotail dynamics and its impacts on high-latitude ionospheric electrodynamics.

Magnetosphere-ionosphere coupling entails the transport of electromagnetic power and mass between the ionosphere-thermosphere and the magnetosphere. The electrodynamic response of the system to changes in solar wind forcing gives rise to changes in convection, in the flow of electrical currents within and between the two regions, and in the dissipation of electromagnetic power, especially in the ionosphere. The inertial interaction involves redistribution of mass and momentum throughout the coupled system and determines, for given solar-wind conditions, the state of convection and current flow. We now recognize that the electrodynamic response is strongly influenced by the inertial response and vice versa, especially for strong solar wind forcing, and that an adequate treatment of the coupling requires a unified approach to modeling.

Stormtime enhancements in the solar-wind electric field are observed to cause 1) deep penetration of the enhanced electric field into the magnetosphere-ionosphere system, which accelerates dense midlatitude plasma of the dayside and entrains it in the high-latitude convection, with the result that 2) substantially elevated parcels of *F*-region plasma enter the cusp, polar cap, and nightside auroral regions (Foster et al., 2005). Collisionless plasma acceleration in these regions, fed by enhanced electromagnetic power flows from the solar wind dynamo, diverts large

fluxes of convecting ionospheric mass into magnetic field-aligned outflows (Moore et al., 1999; Strangeway et al., 2005). Upon reaching the magnetotail, these outflows augment the solar wind population in the plasma sheet. As the energized ionospheric ions join the internal circulation of the plasma sheet come ring current, they are believed to be responsible, in part, for the greatly enhanced stormtime ring current (Daglis et al., 2003). Numerical studies also suggest that the throttled stormtime outflow of heavy ions eventually chokes the storm-enhanced convection by mass loading the magnetosphere (Winglee et al., 2002).

The magnetosphere-ionosphere *feedback* processes manifest in the intensification of the ring current and saturation of polar convection, both attributed to enhanced concentrations of O^+ in the magnetosphere, have yet to be verified observationally or in a fully self-consistent simulation. The second of these processes, namely the effects of heavy-ion outflows on the stormtime electrodynamics of the magnetosphere-ionosphere system, is the primary focus of this project.

Although the modeling studies proposed here do not explicitly address space weather phenomena such as stormtime enhancements in penetrating radiation, thermospheric expansion and satellite drag, scintillations of trans-ionospheric radio signals, or generation of ground-induced currents in electrical transmission systems, the proposed improvements in modeling are absolutely critical elements in the physics-based modeling approach to numerical space-weather forecasting of these phenomena. The processes of magnetosphere-ionosphere coupling in effect embody the “communication and transportation networks” that enable the “globalization” of geospace during storms.

1.2 Technical Approach and Methodology

To address our primary science issues, we will utilize the Coupled Magnetosphere-Ionosphere-Thermosphere (CMIT) model developed by the Center for Integrated Space Weather Modeling (CISM). As currently implemented, the CMIT model electrodynamically couples the one-fluid version of the Lyon-Fedder-Mobarry (LFM) global magnetospheric model (Lyon et al., 2004) to the NCAR Thermospheric-Ionospheric Nested Grid (TING) model. This coupling provides a causal specification of precipitation and convection from LFM for driving TING

(Wang et al., 2004); in return TING provides a more accurate specification of the ionospheric conductivity for use in closing the field-aligned current at the LFM ionospheric boundary (Wiltberger et al., 2004). The CMIT model will be extended here to encompass a recently implemented multifluid version of the LFM code and model sources of ionospheric outflow.

The multifluid extension of the one-fluid LFM model treats the dynamics of three ion species – ionospheric O^+ and ionospheric and solar wind protons – and neutralizing electrons. The multifluid formulation is based on a drift-MHD approach (Kulsrud, 1983) in which all ion species move at the $\mathbf{E} \times \mathbf{B}$ velocity in the perpendicular direction with the parallel motion of each species evolving via its parallel momentum equation, constrained by quasineutrality.

Extensions to the ionospheric boundary conditions of the LFM model have already been implemented to simulate outflows causally driven by EM power flows from the magnetosphere (Gagne, 2005). These boundary conditions will be further advanced under the proposed project. This novel treatment of auroral- and cusp-region outflows makes use of the Strangeway et al. (2005) empirical formula derived from FAST satellite data; the formula relates the outflowing O^+ number flux to the downgoing Poynting flux. Such empirical relations are very much a work in progress (cf. Zheng et al., 2005), and their use in the context of global modeling would benefit from further developments based on a much larger data sample and statistical analysis. Such an investigation would nicely complement our proposed research.

Further extensions of LFM's ionospheric boundary conditions will be implemented in order to model polar wind outflows in a manner similar to that described by Winglee et al. (2002). In this approach, a pressure differential between the ionospheric boundary and the free fluids in the dynamically varying magnetospheric domain causes outflow or inflow.

The major technical challenge and innovation envisioned for this project involves using the TING component of CMIT to dynamically regulate the outflowing ion fluxes (auroral-polar cap boundary region, cusp-region and polar wind) at LFM's low-altitude boundary. TING is a general circulation model and, as currently implemented, does not include inertially forced field-aligned motion leading to transonic flows. But it can be used to specify where ionospheric upwelling and

convective surges modulate otherwise empirically determined (e.g. Strangeway et al.) or pressure-driven, field-aligned flows at LFM's low-altitude boundary. Further details of our methodology are described in Sec. 3 - 4.

1.3 Scientific Impact

The collisionless physics of magnetosphere-ionosphere coupling is a major problem in geospace science – more generally, in the physics of planetary magnetospheres. In addition to the CISM-CMIT project, several other independent efforts are underway to develop and/or advance either a single, continuous simulation model for the geospace medium from the ionosphere up (MRC-ISM) or a hybrid simulation model that couples a global magnetospheric model to a large-scale thermosphere-ionosphere model (CSEM-BATSRUS, UNH-OPEN/GGCM, and NRL-LFM/SAMI3). However, without including the consequences of collisionless ion energization in regions of intense, earthward-directed Alfvénic Poynting fluxes, none of these models, including CMIT, will be able to causally inject the massive ionospheric outflows that occur during major episodic events such as geospace storms and substorms. Without a causal model for ionospheric outflows, accurate prediction of the state of the high-latitude ionosphere and thermosphere is significantly diminished.

The problem is even more profound for the magnetosphere. It is well known that the high-latitude ionosphere is a persistent source of outflowing plasma and essentially the only source of O^+ in the magnetosphere (Yau and André, 1987; Chappell et al., 2000). But are there implications of populating the magnetosphere with ionospheric O^+ that result in fundamentally different system dynamics? Is magnetospheric structure sensitive to the relative rates of supply and distribution of plasma from the solar wind and the ionosphere, or to the mass composition of the magnetosphere? Observation has revealed that the ionosphere does release enormous fluxes of O^+ during active periods, and it is known that ionospheric O^+ can dominate the plasma sheet (Peterson et al., 1981; Kistler et al., 2005) and ring current (Lennartsson and Sharp, 1982; Nosé et al., 2005) during such periods. However, a review of the extensive literature on mass composition (Lotko, 2006) reveals few insights into the global consequences of populating the magnetosphere with an admixture of solar wind and ionospheric plasmas.

New insights into the *electrodynamic* coupling between the solar wind, magnetosphere and ionosphere have emerged from investigations of the integrated system during storm intervals (Ober et al., 2003; Siscoe et al., 2004). Therefore by focusing efforts on the effects of ionospheric outflows on magnetosphere-ionosphere coupling during periods of strong solar wind forcing, we might also expect to improve our understanding of *inertial* coupling and feedback in the solar wind – magnetosphere – ionosphere system.

1.4 Relevance to NASA Programs

The proposed project specifically addresses the primary goal of LWS TR&T Focused Science Topic b) Effects of Ionospheric-Magnetospheric Plasma Redistribution on Storms, which aims “to establish how the magnetospheric uptake of ionospheric plasma during storms changes as a result of plasma restructuring, and how this uptake influences the dynamics and coupling of the magnetosphere and ionosphere.” A detailed research plan to address these issues is described in subsequent sections.

The project is also well-aligned with NASA’s 2006 Strategic Plan, in particular, Sub-goal 3B: Understand the Sun and its effects on Earth and the solar system, for which a primary objective is to understand and predict the causes of space weather by studying the Sun, the heliosphere, and planetary environments as a single, connected system. Although the proposed research does not encompass the physics of the sun or the interplanetary medium, it does significantly advance the state-of-the-art in treating the magnetosphere-ionosphere-thermosphere as a single interacting system including both electrodynamic and inertial coupling.

The current Roadmap for Heliophysics Science and Technology 2005-2035 recognizes that “the exchange of mass and energy [that couple the inner and outer regimes of geospace] during both quiescent conditions and disturbed times must be understood before predictive capabilities, or strategies to mitigate adverse space weather effects, can be developed.” This project directly addresses the need to understand and to develop improved modeling capabilities for the exchange of mass between the inner and outer regions of geospace. This particular aspect of global modeling heretofore has significantly lagged the modeling of electrodynamic energy exchange and coupling.

Because the mass composition of the magnetosphere is a primary observational diagnostic of many geospace satellite missions, it is imperative that we develop modeling capabilities to facilitate the interpretation of such measurements, particularly when combined with conjunctive observations from other regions of geospace. In this regard, the proposed research will directly support existing NASA missions such as Cluster, Polar, and FAST, which include mass composition measurements. It also anticipates the science goals of future missions such as THEMIS, TWINS, MMS, Radiation Belt and I-T Storm Probes, and Global Electrodynamic Connections and will provide an important touchstone for the science derived from them.

2 Science Issues

2.1 Ionospheric Convective Transport

Storm-enhanced transport of dayside ionospheric plasma from mid- to high-latitudes is a consequence of at least two coincident conditions: 1) an inflated mid-latitude *F* region caused by the penetration of stormtime electric fields at low latitudes (Kelley et al., 2004); and 2) enhanced convection and entrainment of the mid-latitude dayside ionosphere in the polar circulation pattern (Foster et al., 2004). These conditions produce a plasma convective surge that flows toward the dayside convection throat from mid-latitudes. The phenomenon may be observationally visualized by projecting “instantaneous” maps of total electron content (TEC) derived from ground GPS receivers onto a “simultaneous” snapshot of the global convection pattern inferred from SuperDARN measurements (Foster et al., 2005). The TEC “snapshot” of a surge, or “tongue of ionization” (Sato, 1959; Sojka et al., 1993), shown in Fig. 1 was taken about 2 hours after its leading edge first entered the dayside cusp, nominally located at 70-75° latitude. It carries 10^{26} ions/s from the mid-latitude ionosphere into the convection throat (Foster et al., 2004).

The TEC values are seen to be largest in the mid-latitude dayside region and progressively decrease, with some variability, along the convective path as the plasma moves across the polar cap from dayside to nightside. The weak antisunward gradient in TEC over the polar cap may arise from the divergence of streamlines evident in Fig. 1. Plasma diffusion enhanced by gradient-drift instabilities (e.g., Sojka et al.,

1998a) may also play a role, although the fast storm-enhanced convection appears to maintain the integrity of the large-scale surge as it traverses the polar cap.

The topside plasma density decreases in and poleward of the cusp where the convecting F -region plasma is diverted into field-aligned outflows, to be modeled as described in Sec. 3. Note that these outflows continue to contribute to the TEC until they reach several R_E altitude, at which point they are above the line of sight of the GPS satellites used to infer TEC. Thus the reduction in the topside density is not as evident in TEC maps as in incoherent scatter radar data (Foster et al., 2005).

Time-sequenced TEC-convection maps like the snapshot shown in Fig. 1 have made it abundantly clear that the global pattern of ionospheric plasma transport is strongly modulated during storms. Observations (Moore et al., 1999) and models (Sojka et al., 1998b) have also verified that polar outflows are strongly modulated during storms. However, we have little reliable knowledge regarding the impacts of these outflows on the magnetosphere and their implications for magnetosphere-ionosphere system dynamics when the magnetosphere is loaded with ionospheric plasma, particularly heavy ions. A

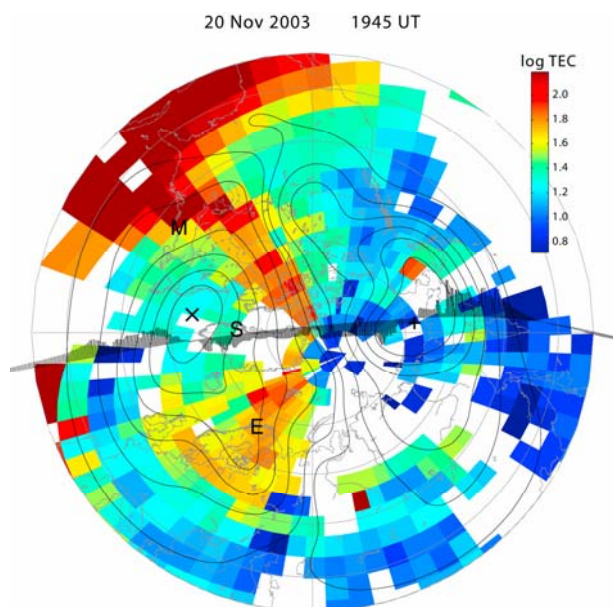


Fig. 1. TEC map of a storm-induced tongue of ionization about 3 hours after the convective surge began transporting enhanced F -region plasma poleward from the midlatitude dayside (Foster et al., 2005).

compelling need exists to improve our capabilities to diagnose and analyze these impacts.

2.2 Magnetospheric Impacts of Outflows

Ionospheric outflows contribute mass, momentum and energy to the magnetosphere. Inside the lobes, during disturbed times, ionospheric O^+ ions appear as quasi-field-aligned, nearly monoenergetic beams, propagating antisunward from the ionosphere (Sharp et al., 1981; Seki et al., 1998; Sauvaud et al., 2004). High-time resolution measurements from the Cluster satellites have shown that H^+ , He^+ , and O^+ ions are injected into the tail during substorms from the nightside ionosphere, with a single injection accounting for over 80% of the oxygen population of the midtail plasmashet during storms (Sauvaud et al., 2004). Oxygen can dominate the energy density of the ring current during storms (Nosé et al., 2005) and both the local number and energy densities of the plasmashet during stormtime substorms when the outflow rate is high and convection is strongly enhanced (Kistler et al., 2005). The outflow rate of superthermal ions increases monotonically with increasing solar-wind power, especially strongly for O^+ , with some indications that solar-wind kinetic power ($\frac{1}{2}\rho_{sw}v_{sw}^3$) may be more essential than EM power ($\mu_0^{-1}\mathbf{E}_{sw}\times\mathbf{B}_{sw}\cdot\hat{x}$) for mass extraction (Lennartsson et al., 2004).

An early review of models and observations by Daglis and Axford (1996) suggested that an O^+ -rich plasmashet influences the onset of substorm expansion and its tailward location by modifying the stability properties of the plasmashet, while an O^+ -rich ring current supports larger amplitude storms, with the rapid initial recovery characteristic of great storms attributed to the rapid loss of O^+ ions via charge exchange in the inner ring current. However, a more recent examination (Peterson, 2002) of data and models was unable to validate the hypothesis that higher abundances of O^+ in the plasmashet initiate plasma instabilities leading to substorm onset. For some storms, flow-out loss of the partial ring current to the magnetopause, combined with compositional changes of the plasmashet source, may account for a substantial part of the initial fast decay of a two-stage recovery (Liemohn et al., 2001). If the increase in the ratio of O^+/H^+ energy density of the ring current with increasing Dst (Nosé et al., 2005) is a consequence of storm-enhanced O^+ outflows first populating the plasmashet and inner magneto-

sphere, and eventually the ring current, then the causality for storms is not entirely clear either: Does an O^+ -rich ring current make big storms or do big storms make the ring current O^+ -rich?

An H^+/O^+ admixture in the magnetotail not only has the potential to modify stability properties, but also the rate and distribution of reconnection. Shay and Swisdak (2004) find that the reconnection rate in a 2D, three-species fluid simulation is about 2/3 the rate in a two-fluid plasma. Given the simulation condition, $m_{O^+}n_{O^+} \gg m_Hn_H$, which is satisfied during the storm-substorms reported by Kistler et al. (2005), they speculate that the expansion phase of substorms may take longer and will reconnect less lobe magnetic flux in the same amount of time. An immediate implication is an increased demand for episodic unloading of magnetotail flux culminating in substorms of increasing intensity. The slower reconnection rate of an O^+ -rich plasmashet cannot quasi-statically balance dayside reconnection for steady upstream conditions. This imbalance must be exacerbated with each subsequent substorm, which adds more O^+ to the magnetotail.

The delivery of interplanetary magnetic flux to the dayside must therefore be dynamically curtailed via some form of feedback that signals the magnetotail's inability to reconnect lobe flux fast enough. Thus far we have no evidence that the dayside abundance of O^+ approaches that of the plasmashet, so the addition of heavy ions to the dayside may be insufficient to limit the dayside reconnection efficiency, at least via a process similar to that in the Shay-Swisdak simulations. The maximum stormtime O^+ density near the dayside magnetopause (Bouhram et al., 2005) is evidently about $1/4$ that of plasmashet (Kistler et al., 2005).

2.3 Electrodynamic and Inertial Coupling

Global MHD simulations provide some insights into the response of the MI system to this crisis. The force exerted on the magnetosheath flow in its interaction with the dayside region 1 currents is normally weak in comparison with the Chapman-Ferraro currents. However, for the large solar-wind electric fields accompanying storms, unusually intense currents are induced by storm-enhanced convection. The global simulations suggest that the magnetic field produced by these currents deflects a portion of the upstream flow and frozen-in magnetic flux before it reaches the magnetopause (Merkine et al.,

2003; Siscoe et al., 2004). This purely electrodynamic effect may be further enhanced by the diversion of an O^+ -inflated ring current into region-2 currents, most of which must be closed through the ionosphere by the dayside region-1 currents. One manifestation of this effect is a nonlinear saturation of the transpolar potential (Russell et al., 2001; Hairston et al., 2005).

Winglee et al. (2002) assert that the transpolar potential is also influenced by the presence of heavy ions in the magnetosphere. In a series of multifluid global simulations of the 24–25 September 1998 magnetic cloud event, they found that the simulated potential more closely matched that calculated from the AMIE data assimilation model when the ion fluence at their inner boundary was chosen to match the statistical rate reported by Yau and André (1997), with a 50/50 O^+/H^+ abundance at the boundary. For lower outflow rates, or outflow without oxygen, the simulated transpolar potential was found to be unrealistically large. The power dissipated by the accelerated O^+ outflow was also found to be substantial in the simulations, on the order of 100 GW, for sustained southward IMF.

Winglee et al. assert that this effect is a consequence of inertial loading of convection by the storm-throttled polar outflow, which eventually chokes the convection, thereby saturating the transpolar potential. What is not clear in this picture is how the dynamics of convection and centrifugal acceleration of ions in the lobes (Cladis, 1986) modify the lobe pressure which must regulate the thermal outflow and, therefore, the mass addition at the low-altitude boundary.

The electrodynamic effects described by Siscoe et al. (2004) modify the external flow and reduce the magnetic flux delivered to the dayside, in contrast with the inertial effects described by Winglee et al. which seem to act entirely internally. It is difficult to compare and assess the relative contributions of electrodynamic and inertial feedback in the two approaches. In one set of models (one-fluid MHD), the ionospheric electrodynamic effects are a major factor in regulating the solar wind-magnetosphere coupling, with the solar-wind dynamo supplying ~ 100 GW to ionospheric Joule dissipation; however, the inertial loading associated with ionospheric outflow is completely absent in these models. In the multifluid model of Winglee et al., the ionospheric electrodynamic effects are passive while ionospheric outflow and centrifugal acceleration of O^+ over the polar cap draw ~ 100 GW

from the solar wind dynamo. A composite model that includes realistic electrodynamic and multispecies inertial coupling between the magnetosphere and ionosphere is clearly needed to resolve these issues. Our aim is to develop such a composite model, which will allow us to answer the primary science questions motivating the investigation (Sec. 1.1).

3 Modeling Outflows in MI Coupling

The character of high-latitude outflows, and the acceleration that enables ionospheric ions to overcome gravity, varies along the ionospheric convection path. Although the theory of these acceleration processes is incompletely understood, we can make use of recent observational results to model causal effects. The dayside cusp and the nightside auroral-polar cap boundary regions corresponding, respectively, to the low-altitude projections of dayside and nightside reconnection activity exhibit intense Alfvén-wave turbulence, ion transverse heating and upward field-aligned ion flows. These outflows feed the high-altitude cusp/cleft region (Lockwood et al., 1985; Bouhram et al., 2004) and the plasmashet (Tung et al., 2001), respectively. In the main auroral zone, one finds upward ions energized by parallel electric fields associated with inverted-V precipitation regions and upward field-aligned currents, and outflowing conic distributions energized in downward current “pressure cookers” (Gorney et al., 1985; Lynch et al., 2002). These latter sources also feed the plasmashet. At higher latitudes, a thermal polar wind expands into the low-pressure lobe/mantle from the polar cap (Banks and Holzer, 1968).

The plasma of the corotating plasmasphere presents a special problem and cannot be realistically treated in the context of the large-scale modeling approach to be employed here. This shortcoming is a feature of the current state-of-the-art in global modeling and is present in all existing global models encompassing the magnetosphere. Several separately funded and independent initiatives are underway by various groups to remedy this problem. We will be opportunistic in making use of such model improvements as they become available, as well as in any other areas where model and code innovations have the capacity to advance project goals.

The quiet-time and active polar wind is always a significant source of outflowing thermal plasma (Chappell et al., 2000), and outflows

from the cusp and auroral/boundary polar-cap regions are especially important during storms. We first describe our approach to modeling superthermal ion energization and outflow in the latter regions (3.1), followed by a description of how we will model polar-wind outflows (3.2). By most estimates, these outflows produce the bulk of O^+ that reaches the magnetosphere during active periods (e.g., Yau and André, 1987).

3.1 Cusp- and Auroral-Region Outflows

The production of intense fluxes of outflowing superthermal ions requires two principal ingredients: 1) a high-density topside source plasma, which may be produced in several different ways as described below; and 2) a source of electromagnetic power cascading to the extreme low-frequency regime where efficient wave-ion energy transfer occurs (Lund et al., 2000). These two quantities will be derived from the CMIT model. The state of the ionospheric source plasma will be derived from the TING component of CMIT while the electromagnetic power flowing into ionospheric source regions from magnetospheric dynamos will be derived from its LFM component.

The altitude of production of intense outflows is not known precisely and may vary with the particular wave-particle interactions involved. Most of the microscopic wave-particle interactions that produce transversely accelerated ions break the first adiabatic invariant. Because the ion gyroradius and gyroperiod increase with altitude, the mechanisms that produce transverse ion acceleration prefer relatively high altitudes. However, if the altitude of the energization region is too high, few ions will be energized because the density of the ionospheric source plasma decreases with altitude and will be relatively low. Variations in wave propagation characteristics with ambient properties also complicate an assessment of the optimum altitude for energization (Johnson and Cheng, 2004). After attaining sufficient perpendicular energy, the transversely accelerated ions are propelled upward by the mirror force and escape into the magnetosphere with motion becoming increasingly field-aligned. In any event, the bulk of the ion acceleration leading to outflow occurs above TING’s upper boundary and below LFM’s lower boundary, so we will employ a lumped systems approach in specifying the outflow flux.

The causal relationships between electromagnetic power flowing into a low-altitude energiza-

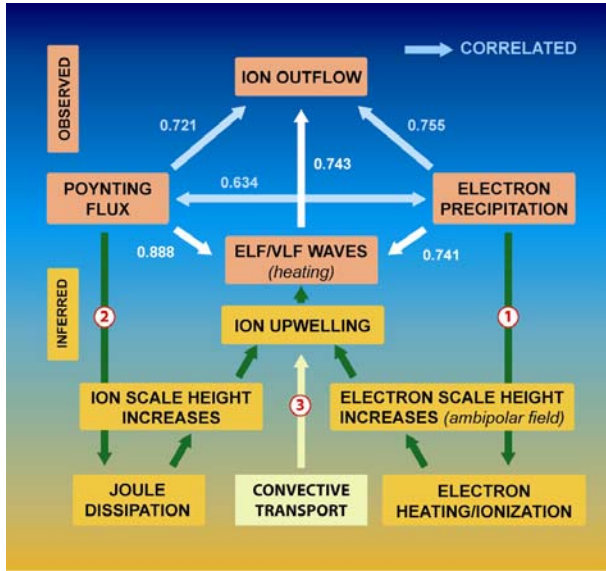


Fig. 2. Causal relationships between magnetospheric inputs and F -region upwelling (adapted from Strangeway et al., 2005).

tion region and the properties of the superthermal ion fluxes flowing upward from it are an active area of investigation. A comparison between empirical studies based on FAST (Strangeway et al., 2005) and Polar (Zheng et al., 2005) satellite data suggest that such relationships may be quite complicated, with hidden or untested variables modifying the relation for different ambient conditions. The transport law undoubtedly depends on both the frequency and wavenumber spectra of the power source and the initial density, stratification, composition and energy of the source plasma. Both DC and time-variable electromagnetic power flows are relevant, but the associated pathways to ion energization can be very different.

Fig. 2 illustrates the interrelationships between various processes leading to ion outflow (Strangeway et al., 2005). The pathways to upwelling and eventually to outflow include: ① an upward ambipolar electric field in regions of enhanced soft (~ 100 eV) electron precipitation, e.g., in the cusp and nightside auroral/boundary polar-cap regions. Soft electron precipitation deposits energy in the F region, increases the upward electron pressure gradient there, and, through the ambipolar field, forces the F -region ions upward, causing upwelling; ② ion frictional heating in the E and lower F layers due to enhanced convection, which increases the bottom-side ion pressure, forcing ions upward, thereby

causing upwelling. Modeling studies (Liu et al., 1995) indicate that soft electron precipitation is usually more effective in producing upwelling than Joule heating. The stormtime TEC-convection maps developed by Foster et al. (2005) suggest an important third way of swelling the topside ion density in the cusp energization region during storm periods, also in the nightside auroral/boundary polar-cap region (Semeter et al., 2003): ③ convection of a parcel of inflated topside ionosphere into an energization region from the midlatitude dayside ionosphere or, in the case of a nightside energization region, from the polar cap.

All three of the above processes leading to upwelling are included in the CMIT model. LFM provides TING with a proxy for the precipitating electron number flux (pathway ①) and the electric field that determines both the ionospheric Joule dissipation rate (pathway ②) and convective plasma transport (pathway ③). These quantities are then used by TING to adjust the ionization state of the ionosphere and its stratification.

While the low-altitude cusp and cleft regions are evidently the most persistent sources of magnetospheric O^+ , accounting for about 1/3 of the total O^+ outflow during quiet times at solar minimum (Peterson et al., 2005), the nightside auroral-polar cap boundary region produces the most energetic and largest peak fluxes of O^+ outflows during active periods (Tung et al., 2001). The electromagnetic power flows that energize ions in the topside ionosphere and low-altitude magnetospheric regions immediately equatorward of the polar cap boundary are generated in magnetotail dynamos, in contrast with low-altitude cusp energization which is electro-dynamically connected to dayside and magnetopause boundary layer dynamos.

Despite the different dynamo sources, the low-altitude energization processes themselves are quite similar (André et al., 1998; Chaston et al., 2004; 2005). We will use a single transport model to specify the outflow rate resulting from such processes regardless of their location, e.g., in the auroral, cusp, or polar cap regions. The model will be based on empirical relations similar to the one shown in Fig. 3, wherein the ion outflow flux in ions/cm²-s is given by $F_i = 2.14 \times 10^7 S_{\parallel}^{1.265}$ with Poynting flux S_{\parallel} in mW/m². Lumped transport models of this form are well-suited to specifying the ion fluxes through the lower boundary of the LFM simulation model given the numerically computer Poynting flux at

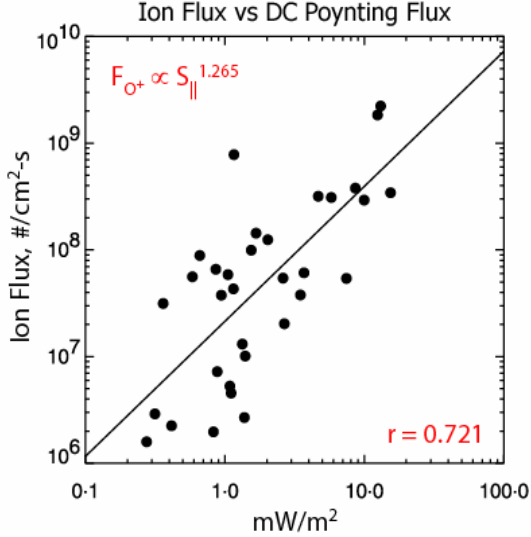


Fig. 3. Correlation of outflowing ion flux (dominantly O^+) with downgoing Poynting flux from FAST data (Strangeway et al., 2005).

the boundary. We will experiment with different forms of this relationship for H^+ and O^+ , using observational constraints as proposed by Strangeway et al. (2005), Zheng et al. (2005), and others as they become available, to explore their impacts on the outflowing ion flux.

The schematic in Fig. 2 indicates that both EM power flow to low altitudes and an elevated or upwelled topside ionosphere are necessary for the development of intense stormtime outflows. One approach to modeling causally-driven outflows regulated by both the EM power supply and an enhanced ionospheric source population is illustrated in Fig. 4 from Gagne (2005). This model uses the Strangeway et al. (2005) empirical formula to specify the outflowing ion flux given the downflying Poynting flux derived from the LFM computation. However, before releasing Strangeway’s outflowing ion flux through the low-altitude LFM boundary, Gagne multiplies the flux by a “mask” function, specified in his formulation as a simple top hat function derived from LFM’s proxy for the precipitating electron number flux (the top hat function is constant when the flux exceeds a critical value and proportional to the flux when less than the critical value). In using information about the precipitating electron flux, Gagne is effectively regulating the outflowing ion flux by convolving it with information about the local state of ion upwelling along the pathway ① described above.

A sample simulation result derived from Gagne’s approach is shown in Fig. 5 for a case

of pure H^+ outflow in a controlled LFM simulation with nominal conditions of $V_{SW} = 400$ km/s and $n_{SW} = 5/cm^3$. The IMF of magnitude 5 nT progressed through 3 constant states over a 12 hour period, 3 hours each pointing northward, then eastward, then southward. The outflow at the boundary was turned-on when the IMF rotated southward. The plot shows the H^+ outflow flux at the inner simulation boundary at the end of the 4-hour period of southward IMF. The cusp-region outflow is evident. The relatively weak nightside outflow is a consequence of the fact that the magnetotail is not very active for the chosen solar wind driver. The fairly intense outflows near dawn and dusk are an artifact of Gagne’s algorithm (and perhaps Strangeway’s empirical formula) which tends to emphasize regions where intense DC Poynting flux flows into the ionosphere from the LFM domain. The intense dawn and dusk outflows occur where i) LFM’s proxy for precipitating electron flux is appreciable (the influence of Gagne’s “mask” function), and ii) the simulated region 1 and region 2 currents close via ionospheric Pedersen

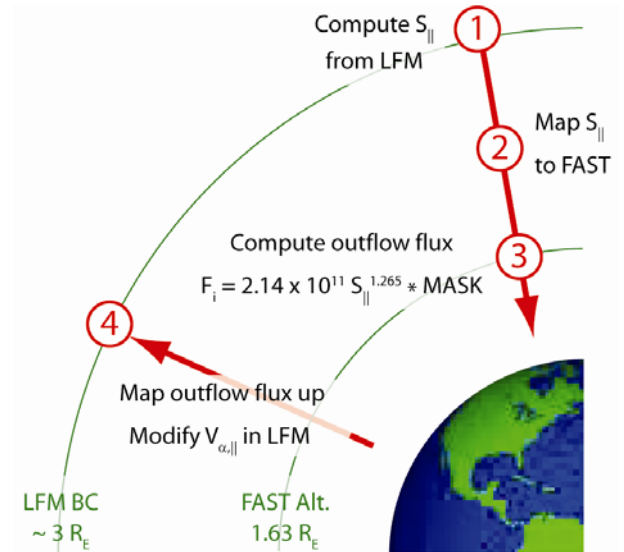


Fig. 4. Gagne’s algorithm ingests the mapped Poynting flux at the LFM inner boundary into Strangeway et al.’s empirical formula for O^+ outflow flux, multiplies the result by a “masking function” derived from the LFM proxy for precipitating electron number flux, and maps the resulting outflow flux upward to specify the boundary condition at LFM’s boundary. In our approach, Gagne’s masking function will be replaced by a prognostic function derived from TING’s calculation of the topside ion density.

currents, with the implied Joule dissipation being fed by fairly intense Poynting fluxes from the magnetosphere (Olsson et al., 2005).

We will replace Gagne’s masking function, which is based purely on the electron precipitating flux, with a more sophisticated prognostic function for the topside source density derived from the TING component of the CMIT model. TING’s physically richer and more realistic ionospheric state reflects local changes in the topside density attributed not only to electron precipitation but also to dynamic ion Joule heating and convective transport of ionospheric parcels from nearby regions where the *F*-region density may be different. As discussed in Sec. 4.2, TING has the capacity to generate a polar tongue of ionization when driven by storm-enhanced convection. This prognostic function will be convolved with the empirically specified function relating outflow flux to Poynting flux, e.g., Strangeway et al. (2005). Use of a prognostic function derived from the TING model to represent the influence of a variable ionospheric source population for the outflow should moderate the non-causal artifacts resulting from Gagne’s more primitive model.

3.2 Polar Outflows and Inflows

The stormtime polar wind exhibits consider-

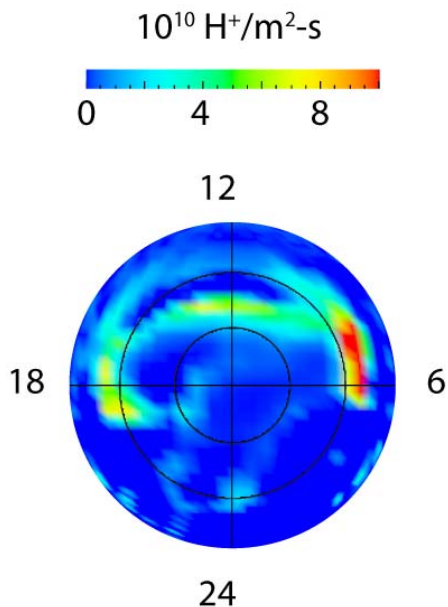


Fig. 5. Sample result for H^+ outflow resulting from Gagne’s algorithm for the low-altitude boundary condition in the LFM model. The outermost circle corresponds to 60° ILAT.

able structure in space and time (Schunk and Sojka, 1997) and can be dominated by O^+ (Yau and Andre, 1997), in contrast with the non-stormtime polar wind which, statistically, is an H^+ polar wind, at least near solar minimum. At solar maximum an elevated topside density resulting from enhanced solar EUV fluxes sustains larger O^+ thermal outflows relative to the solar-minimum average (Cannata and Gombosi, 1989; Abe et al., 2004). The increase in O^+ outflow from solar minimum to maximum conditions is much greater than the relative increase in H^+ outflow, thereby resulting in higher concentrations of O^+ in the polar wind at solar-maximum (Cully et al., 2003). The processes responsible for producing the polar wind are present at essentially all latitudes, including those in and equatorward of the auroral zone; however, the associated outflow is substantially modified from the “classic polar wind” at nonpolar latitudes by wave-particle interactions and outflow-limiting boundary conditions.

Winglee et al.’s (2002) simulations of the magnetosphere, including polar wind-like O^+/H^+ outflows and simple ionospheric electrodynamics, are an important reference point for the project proposed here, so we will review Winglee’s treatment of the ionospheric boundary conditions before describing our modeling approach to pressure-driven outflows designed to simulate some of the phenomenological features of polar wind outflows as described above.

Ionospheric electrodynamics are simulated in Winglee’s model by introducing a resistive term in the generalized Ohm’s law. The resistivity is constant on the inner simulation boundary and is set to zero two grid cells above the low-altitude simulation boundary located, e.g., at geocentric distance of $2.5 R_E$ in Winglee (2004). Placement of this resistive layer in the computational domain is designed to mimic *E*-region current closure. A finite tangential electric field is thus permitted at the boundary, which serves as a proxy in Winglee’s simulations for the high-latitude potential distribution.

Winglee notes that his admittedly crude approximation for the ionosphere is ameliorated to some extent by inertial-loading of convection by heavy ion outflows. He asserts that these outflows tend to counteract dynamic increases in the ionospheric conductivity, rendering the details of conductivity dynamics less important when heavy ion outflows are present. His point is well-taken that the response of the regionally

coupled MI system also involves physical couplings between electrodynamic and inertial effects. One of the primary objectives of this project is to investigate this assertion in the context of the physically more comprehensive ionospheric model of the standalone, multifluid LFM model, as well as in the CMIT model with multifluid extension of its LFM component.

Depending on the particular physical application and location on the inner boundary, Winglee sets the boundary condition on the plasma density there in the range of 10^2 - 10^3 cm^{-3} . The composition at the inner simulation boundary (O^+/H^+ density ratio) is also fixed in time, with different ratios heuristically specified. The ion pressure (as well as density and temperature) are fixed in time at the inner simulation boundary, with local flux-tube equilibrium initially ensured by requiring a constant pressure distribution along each field line.

As with all global simulations of the magnetosphere, numerical constraints require the inner simulation boundary to be placed well above the altitude of significant gravitational pull on the ions. Winglee artificially increases the mass of the earth to mimic the gravity that O^+ would ordinarily experience in the topside ionosphere. The bulk of the O^+ at the inner boundary is thereby gravitationally bound. H^+ and O^+ field-aligned flows arise at the inner boundary (in or out) when the species pressure in the dynamic simulation domain varies relative to the species pressure on the boundary.

Winglee's results provide a useful touchstone for our proposed studies, and, initially, we will follow his boundary specifications fairly closely. In this context, we will begin to investigate the interplay between inertial MI coupling stimulated by polar wind-like, pressure-driven outflows and the more faithfully representative ionospheric electrodynamics of the CMIT and standalone LFM models. Subsequently we will incorporate pressure-driven outflows specified in this way with empirically specified outflows representing the collisionless auroral- and cusp-region processes described in the previous subsection. At this juncture we will be in a position to begin to evaluate the relative importance of the two types of outflow processes on magnetosphere-ionosphere coupling.

Given information on the topside ionospheric state available from the TING component of CMIT, the idea of utilizing transonic polar wind solutions extending through the gap region to

connect TING's upper boundary condition to LFM's lower boundary condition seems within reach. Quasi-equilibrium polar-wind solutions of varying degrees of sophistication could be spliced between the TING and LFM boundaries to provide a more realistic connection between the dynamic states of the ionosphere-thermosphere and the magnetosphere. A simpler, heuristic approach might simply use information from TING's ionospheric state to dynamically regulate the pressure distribution at LFM's inner boundary. Given the resources available for this Focused Science Topic, the latter approach is more tractable and will be pursued in the latter stages of the project.

3.3 Other Outflows

At least three types of outflows, of varying degrees of importance during storm periods, are not included in the modeling efforts described above. These include: 1) upward flowing ion beams accelerated by the upward-directed parallel electric fields typically found in "inverted-V" precipitation regions accompanying large-scale, upward field-aligned currents; 2) ion conic outflows produced in downward-current "pressure cookers" (Gorney et al., 1985; Lynch et al., 2002); and 3) convective entrainment of plasmaspheric ions and associated development of plasmaspheric plumes, which occurs in general when the strength of magnetospheric convection is on the rise (Grebowsky, 1970; Goldstein, 2006).

Of the three "other" outflows, auroral ion beams may be the least important during storms in a relative sense. As an example, data from FAST orbit 1906 obtained during a substorm expansion (cf. Fig 4.2 of Paschmann et. al., 2003) shows an Alfvénic region near the nightside polar cap boundary with outflows exceeding 10^{12} ions/ m^2 -s, downward current regions with outflows reaching about 5×10^{11} ions/ m^2 -s, and inverted-V regions with outflows typically less than about 10^{11} ions/ m^2 -s

It is not known in a statistical sense how much plasmaspheric mass is convectively entrained during storms relative to that released from downward-current pressure cookers or from ion beams flowing upward from inverted-V regions. However, plasmaspheric composition is dominantly H^+ (Lemaire and Gringauz, 1998), which may diminish its global impact on the magnetosphere. Given the statistical results of Yau and André (1987), Tung et al. (2001), and

Huddleston et al. (2005), among others, it seems plausible that the outflows described in the previous sections encompass the bulk of the ionospheric mass, certainly the heavy-ion contributions, reaching the stormtime magnetotail and plasmashet.

At this juncture, we have chosen simply not to include these “other outflows.” On one hand, we know so little about the global effects of the outflows we have chosen to model that any knowledge derived from those studies is likely to be significant. Furthermore, when charting new territory, it seems prudent to proceed systematically and somewhat incrementally without turning all simulation “knobs” simultaneously.

4 Global Models

We plan to use the Coupled Magnetosphere-Ionosphere-Thermosphere (CMIT) model for geospace as the primary tool for this study. It provides a framework for modeling the interactions between the solar wind and the magnetosphere-ionosphere-thermosphere system. Here we provide a brief overview of the main modules that make up CMIT—the Lyon-Fedder-Mobarry global magnetosphere (LFM) model and Thermosphere Ionosphere Nested Grid (TING) model. This description highlights features of the models that are essential to the coupling and the study of ionospheric outflow. We also briefly summarize how the models are coupled to form CMIT and where outflow models may be added.

4.1 LFM Global Magnetospheric Model

The LFM code solves the ideal equations of one-fluid magnetohydrodynamics for the interaction between the solar wind and magnetospheric plasmas (Lyon et al. 2004). The primary computational technique is explicit, finite volume MHD. Finite volume techniques for the handling of hyperbolic systems of equations are much more robust and accurate than any of the alternatives that have been applied to MHD. The code uses Adams-Bashforth time marching with a centered eighth-order spatial differencing. In addition, non-linear numerical switches based on the Partial Donor Method (Hain, 1987) are used to maintain a total variance diminishing (TVD) solution. Because the field topology in MHD is so important, special methods have been developed to fulfill this TVD condition for the system of equations while still maintaining the zero nu-

merical divergence of the magnetic field.

The finite volume techniques described above allow LFM to complete the calculation on a numerical grid of nonorthogonal cells adapted to the magnetospheric problem, i.e. cells that are smaller across the nominal bow shock than parallel to it. This makes it difficult to state a single value for the numerical resolution. However, in the inner magnetosphere at low resolution the typical cell size is approximately $1/8 R_E$. The ideal MHD equations do not include the effects of resistivity, which means theoretically that reconnection is not possible. However, the discretization of the equations onto the grid results in a 'numerical' resistivity which allows reconnection to occur in regions where oppositely directed magnetic fields are forced into a single cell. Fedder et al. (1987; 1995) have shown that the rate of reconnection in the magnetosphere is controlled by the solar wind conditions and the coupling with the ionosphere and not by the cell sizes in the simulation.

The standalone LFM model includes an ionospheric model which is coupled to the magnetospheric calculation. A sphere centered on the Earth is removed from the computational domain. The choice of radius of this boundary is governed by two effects: 1) because the Alfvén speed rapidly increases with decreasing altitude, the Courant condition for numerical stability requires the maximum time step to become increasingly smaller when this spherical boundary is placed closer to the Earth; and 2) alternatively, with boundary located closer to the Earth, the computational domain includes a larger extent of the high-latitude ionosphere because lower L-shells map to lower latitudes. In our experience, a sphere of radius $2 R_E$ provides an excellent balance between these two constraints. The field-aligned currents (FAC) flowing at the inner boundary are mapped quasi-statically along dipole field lines to the ionosphere where current continuity and the ionospheric Ohm’s law are applied to obtain the familiar two-dimensional electrostatic relation, $\nabla_{\perp} \cdot \Sigma \cdot \nabla_{\perp} \Phi = J_{\parallel}$, where Σ is the conductivity tensor, Φ is the electric potential in the ionosphere, and J_{\parallel} is the FAC. The electric field determined by this relationship is dipole-mapped to the inner boundary, either ideally or via the Knight current-voltage relationship (Gagne, 2005), for use in the boundary condition on the plasma flow velocity at the inner grid of the LFM magnetospheric solution.

The ionospheric module includes two sources

of ionization that regulate the Pedersen and Hall conductivities represented in Σ : solar EUV radiation and electron precipitation in the auroral region. The LFM algorithm includes a series of empirical models which transform the MHD sound speed and density into a characteristic energy, ε , and flux, F , of the electrons precipitating into the ionosphere (Fedder et al. 1995). The standard LFM ionospheric module converts these parameters into Pedersen and Hall conductances using the empirical relationships derived by Robinson et al. (1987).

Multifluid Extension of LFM

The multifluid LFM code shares similarities with previous work, but does have some significant differences. The only global simulations for the Earth have been developed by Winglee (1998a; 1998b; 2004). However, global multifluid studies have also been reported, for example, for Mars (Liu et al, 1998) and Titan (Nagy et al., 2001; Craven et al., 1998). In these latter cases, each of the species has its own continuity equation, but a single momentum equation is solved for the bulk flow. All species therefore move at the same speed both along and across the magnetic field. In the Liu and Nagy papers a single energy equation is used for all the species. The equations are written in conservative form, thus allowing easy treatment of shocks. The Craven et al. (1998) model uses individual pressure equations to keep track of the thermal evolution of individual species. By contrast, Winglee has used non-conservative equations for the primitive variables that allow for individual species to move relative to one another. In earlier formulations (Winglee, 1998a; 1998b), he assumes that all the species move with the same perpendicular velocity, while in a more recent formulation (Winglee, 2004), he has allowed for individual species to have different cross field velocities. The disadvantage of this approach is that use of the non-conservative equations makes treatment of discontinuities, such as shocks, relatively difficult.

The multi-fluid LFM builds upon the techniques used in the standard one-fluid LFM (Lyon, et al., 2004) to provide a multi-fluid code which is conservative, allows each species to move under its own force balance, and can handle shocks in individual species. In what follows quantities without subscripts refer to averages over the sum of species; individual species are identified by a Greek subscript. The multifluid

LFM code solves the following equations:

$$\begin{aligned} \frac{\partial \rho_\alpha}{\partial t} + \nabla \cdot \rho_\alpha \mathbf{V}_\alpha &= 0, \\ \frac{\partial \rho_\alpha \mathbf{V}_{\alpha,\perp}}{\partial t} + \frac{\rho_\alpha}{\rho} (\nabla \cdot \rho_\alpha (\mathbf{V}_\perp + \mathbf{V}_\parallel) \mathbf{V}_\perp + \nabla P) &= -\frac{\rho_\alpha}{\rho} \mathbf{j} \times \mathbf{B}, \\ \frac{\partial \rho_\alpha \mathbf{V}_{\alpha,\parallel}}{\partial t} + \nabla \cdot [\rho_\alpha (\mathbf{V}_\perp + \mathbf{V}_{\alpha,\parallel}) \mathbf{V}_{\parallel,\alpha}] \\ &+ \nabla_\parallel \left[P_\alpha + \frac{|n_\alpha q_\alpha|}{n_e} P_e \right] = -v_{\alpha\beta} (\mathbf{V}_{\alpha,\parallel} - \mathbf{V}_{\beta,\parallel}), \\ \frac{\partial \mathcal{E}_\alpha}{\partial t} + \nabla \cdot (\mathbf{V}_\perp + \mathbf{V}_{\alpha,\parallel}) \left(\frac{\rho_\alpha}{2} (V_\perp^2 + V_{\alpha,\parallel}^2) + \frac{\gamma}{\gamma-1} P_\alpha \right) \\ &= \frac{\rho_\alpha}{\rho} \mathbf{j} \cdot \mathbf{E}, \\ \text{and } \frac{\partial \mathbf{B}}{\partial t} &= -\nabla \times (\mathbf{V} \times \mathbf{B}). \end{aligned}$$

The first four equations evolve mass continuity, perpendicular and parallel momentum, and plasma energy, $\mathcal{E}_\alpha \equiv \frac{1}{2} \rho_\alpha v_\alpha^2 + P_\alpha / (\gamma - 1)$, for each species. The final equation is Faraday's Law for ideal MHD. The equation for the parallel momentum shows that the ideal motion along a flux tube is independent of the other species. The term on the RHS is a phenomenological drag term, which allows coupling between counter-streaming ions when their relative motion gives rise to plasma micro-instabilities. It is similar to an anomalous resistivity term that is added to the induction equation in some models. Ignoring such effects, the ion drag term is set to zero.

The perpendicular momentum equation states that all the species share the same acceleration in that direction. This deserves comment. The result comes from the use of the MHD ordering (Kulsrud, 1983), $\varepsilon \equiv (\Omega\tau)^{-1} \ll 1$ and $R_\alpha/L \ll 1$ where τ and L are system time and length scales, and R_α is the Larmor radius. A straightforward integration over velocity space for the first moment in the perpendicular direction gives

$$\begin{aligned} \frac{\partial \rho_\alpha \mathbf{V}_{\alpha,\perp}}{\partial t} + \nabla \cdot \rho_\alpha \mathbf{V}_\alpha \mathbf{V}_{\alpha,\perp} + \nabla_\perp P_\alpha \\ = -\frac{\rho_\alpha q_\alpha}{m_\alpha} (\mathbf{E} + \mathbf{V}_\alpha \times \mathbf{B}). \end{aligned}$$

Note that the Lorentz force term is $O(1/\varepsilon)$ if the rest of the equation is of order unity. Thus, $\mathbf{E} + \mathbf{V}_\alpha \times \mathbf{B} = 0$ to order ε to balance the equation. This implies $\mathbf{V}_{\alpha,\perp} = \mathbf{E} \times \mathbf{B} / B^2 + \varepsilon \mathbf{V}_\alpha^D$, where \mathbf{V}_α^D is a drift velocity, and ε is used simply to indicate ordering. Another consequence is that to the

lowest order (MHD) the perpendicular velocity of each species is the same, $\mathbf{V}_E = \mathbf{E} \times \mathbf{B} / B^2$. One can show that the net effect of the drift term in the Lorentz force is to cause all the species to feel the same acceleration in the perpendicular direction. This acceleration is found by summing over all the species momenta equations. The summed equation has a total magnetic force of $\mathbf{j} \times \mathbf{B}$. The current \mathbf{j} is then obtained from Ampere's Law, eliminating the need to know the individual drifts.

4.2 TING Model

TING is a high-resolution, three-dimensional, time-dependent model of the coupled thermosphere-ionosphere system. It is an extension of the NCAR TIGCM (Roble et al., 1988) used to study mesoscale processes in this system (Wang et al, 1999, Wang et al. 2004). The model solves the coupled equations of mass continuity, momentum and energy for the neutral species and O^+ in the thermosphere and ionosphere. Chemical equilibrium is used to obtain the densities of the other ion species (NO^+ , O_2^+ , N_2^+ , N^+) and the electrons. Future extension to include H^+ is planned. Details of the model can be found in Wang et al. (2004) so we will only provide a brief summary here, concentrating on important features in the coupling of TING with LFM.

The basic grid for TING is a regular latitude-longitude grid extending from -87.5° to 87.5° with 5° steps in latitude and longitude. As the name implies, TING has the capability for using nested grids in the latitude and longitude directions to concentrate resolution in regions of significant interest. The vertical grid extends from 97 km to 500 km with 25 constant pressure levels.

The model has four primary inputs; 1) Solar EUV radiation, parameterized in terms of the $F_{10.7}$ flux; 2) auroral particle precipitation characterized in terms of the characteristic energy and number flux; 3) imposed magnetospheric electric field at high latitudes; and 4) tides from the lower atmosphere. In stand-alone operation these parameters are determined from empirical models characterized by indices like K_p or by the solar wind conditions (Wang et al. 2001).

Along with many other parameters the TING model computes the height-integrated conductances, with the Hall and Pedersen conductivities calculated from first principles. This calculation requires determination of the gyro and collision frequencies for major ion species, O_2^+ , O^+ , and

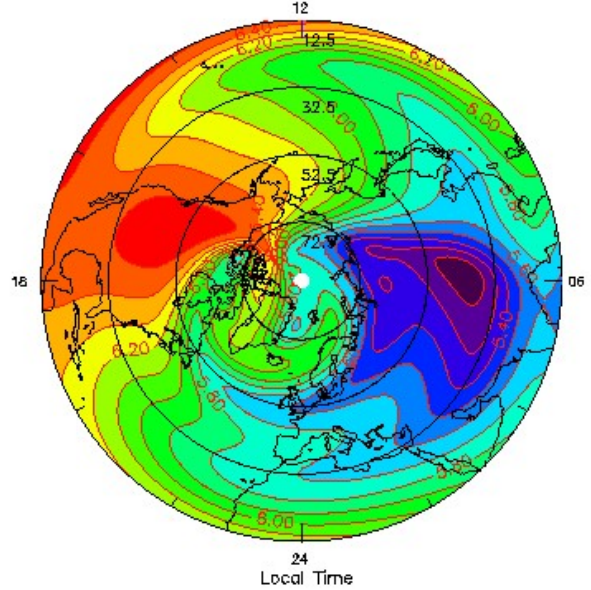


Fig. 7. F_2 -peak electron density showing the formation of a polar tongue of ionization in a nested grid solution from TING (Wang et al., 2005).

NO^+ , as well as the electrons and neutrals.

Wang et al. (2005) have shown that high-resolution solutions obtained from TING's nested grid approach allow it track small-scale ionospheric features not seen at low resolution. Fig. 7 shows the electron densities at the F_2 peak during a moderate geomagnetic storm. A tongue of ionization resulting from strong transpolar ion convection and enhancement of the mid-latitude source region driven by the geomagnetic activity is clearly seen extending through the ionospheric convection throat.

4.3 CMIT Model and Outflow Extensions

Fig. 8 shows a schematic representation of the coupling process between the LFM and TING models to form the CISM CMIT Model along with extensions to the standard CMIT model that are part of this proposal. The model includes three major components. For the purposes of this diagram, the LFM model is limited to the magnetospheric portion of the simulation domain. The magnetosphere-ionosphere (MI) coupler includes the ionospheric portion of the LFM model and infrastructure for communicating between the LFM and TING models.

The two magnetospheric inputs to TING, auroral particle precipitation and the convection electric field, are provided by the LFM via the MI coupler module. It uses the MHD parameters along with empirical relationships to deter-

mine the flux and characteristic energy of the auroral particle precipitation. The MI coupler then makes an initial determination of the ionospheric electric field and completes the UT dependent transformation of these parameters from the LFM ionospheric grid to the TING grid. It waits for the TING model to complete its first-principles determination of the height-integrated Hall and Pedersen conductivities. Once the conductivities have been determined the MI coupler recomputes the electric field and passes it back to the LFM for use as part of its boundary conditions.

The CMIT model has been constructed using the CISM coupling framework [Goodrich et al. 2005] which makes it straightforward to add additional models to the geospace simulation. As illustrated in Fig. 8 the core of the CMIT model includes the LFM and TING models and the MI coupler. We can replace the one-fluid version of LFM with the multifluid version by implementing the transfer of MHD information from the multifluid LFM code via the MI coupler. The auroral/cusp and polar wind outflow models will have standings similar to the MI coupler in the CISM framework. Basically, they will take inputs from LFM and TING and apply the physics of their domains to produce additional boundary-condition information. It is envisioned that the auroral/cusp outflow model will acquire Poynting flux from LFM and combine it with information on the source densities of the various species from TING to compute the distribution of ion flux flowing into the MHD domain. The

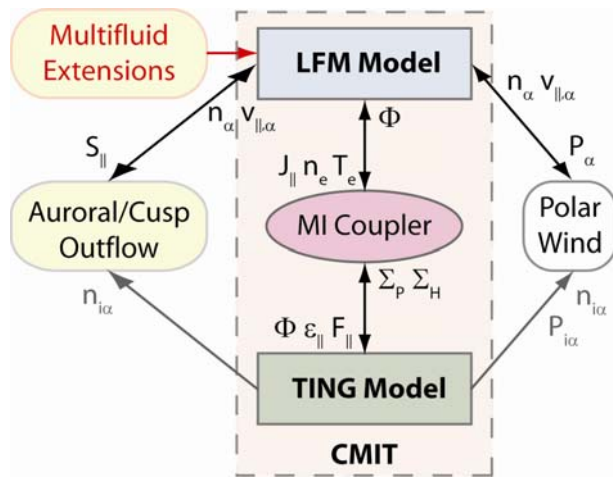


Fig 8. Coupling schematic for the LFM and TING models, the CMIT MI coupler, and information flow through outflow models.

polar wind model will work in a similar fashion except it will use information about the pressure distributions in each model to compute the outflowing flux of ions. The utilization of the CISM framework will allow us to quickly change the physics in an outflow model without having to significantly modify the core models.

5 Personnel, Institutional Support, Work Plan and Milestones

PI William Lotko and Co-I Michael Wiltberger (Co-I), together with unfunded Collaborators John Lyon and Wenbin Wang, are currently engaged in two collaborative projects closely related to the research described in this proposal. One project is funded by the NSF Science and Technology Centers program as the Center for Integrated Space Weather Modeling (CISM); the other is funded by a NASA Heliophysics Theory Program grant to Dartmouth College. Wang and Wiltberger led the CISM code coupling effort that produced the CMIT model.

W. Lotko's responsibilities for this project as PI include overall direction and coordination of the research project, related activities, and personnel including student(s) associated with the project, and preparation and submission of publications of research results, and progress and final grant reports. The PI is familiar with the LFM model and code and directed the graduate research of John Gagne described in Sec. 3.1, which entailed using the LFM code and modifying its ionospheric boundary conditions. He is also familiar in general terms with the TING and CMIT models. The PI will co-develop and co-implement modifications of the LFM and CMIT codes to include the new outflow boundary conditions described in this proposal, together with diagnostics for analyzing and displaying numerical results derived from the simulation studies. He will also participate in the comparison simulation and observational results.

Co-I M. Wiltberger's responsibilities include co-development and co-implementation of outflow models and boundary conditions to simulate outflows in the LFM and CMIT models and related code development, including diagnostics, as described in the proposal. The Co-I will also be directly involved with the scientific interpretation and publication of scientific results derived from the project and will contribute to the development of progress and annual grant reports. The Co-I is one the leading experts in the

use and continuing development of the LFM and CMIT models. He will be responsible for integrating the multifluid LFM model into the CMIT framework.

Collaborator J. Lyon is the principal architect of the LFM model and its extension to a multifluid basis. He will provide expert advice on the use and modifications of the LFM model and the interpretation of numerical results derived from it for scientific applications.

Collaborator W. Wang will provide expert advice on the use and modification of the TING component of CMIT and the interpretation of numerical results from the TING and CMIT models for scientific applications.

The modest funding of salaries proposed in the budget for the PI and Co-I should not be considered indicative of the level of commitment to these studies or to the level of scientific output to be expected. Indeed a review of the PI's and Co-I's current and pending support statements will reveal research-in-progress on several closely related topics. Some flexibility in salary allocations is desirable. If the research can be advanced more efficiently by a modest reallocation of funds part way through the project, adjustments will be made in the support levels of the various personnel.

This proposal is complementary to, but not dependent on, a proposal to the same TR&T Focused Science Topic submitted by Dr. Viacheslav G. Merkin of Boston University entitled

“Stormtime Magnetospheric Plasma Redistribution Including Heavy Ion Outflows and Impacts on Magnetospheric Region.” That project will also utilize the new multifluid capabilities of the LFM model. However, whereas this project integrates multifluid LFM capabilities into CMIT in order to study effects of outflows on MI coupling, Merkin’s proposal will integrate multifluid LFM with the Rice Convection Model in order to study the impacts of outflows more specifically on the magnetospheric region of the system. We would expect considerable synergy between the two projects if both are selected.

Institutional Support

1. Dartmouth will co-sponsor 4.7% FTE for W. Lotko to pursue project research.
2. NCAR will co-sponsor 2.6% FTE for M. Wiltberger to pursue project research.
3. Dartmouth will cost-share 50% of the tuition budgeted for one graduate research assistant.
4. W. Lotko will spend a nine-month sabbatical in residence at NCAR/HAO collaborating on project-related research with M. Wiltberger and W. Wang starting October 1, 2006, with salary fully covered by Dartmouth.
5. NCAR/HAO will allocate necessary General Accounting Units from the divisional allocation to complete high-resolution numerical studies on NCAR supercomputing facilities.
6. NCAR/HAO can host team meetings for LWS TR&T FST B at no cost to NASA.

Work Plan and Milestones

The entries designated T: or S: in the table respectively indicate “Development *Task*” or “Scientific *Study*.”

YEAR 1 TASKS & STUDIES	YEAR 1 → 2,3 TASKS & STUDIES
T: Integrate multifluid LFM in CMIT	T: Implement polar-wind (PW) outflow BCs on LFM
S: Parametric studies of empirical outflow models	T: Develop PW prognostic functions from TING
T: Develop outflow prognostic functions from TING	S: MI impacts of polar-wind outflows
T: Develop simulation diagnostics to characterize outflows and MI impacts	
S: MI impacts of outflows originating in the cusp and auroral boundary polar-cap regions.	T: Merge empirical and PW outflow BCs
	S: MI impacts of combined outflows
S: Ionospheric ion accessibility and population of the magnetosphere	
S: Storm influences on outflow rates and distributions	
S: Regulation of outflows by solar wind kinetic vs. electromagnetic power (cf. Lennartsson et al., 2004)	
T/S: Pursue possible collaborative opportunities with other focused science topic team members	

6 Team Coordinator Proposal

As with any team effort, the expectation for a TR&T Focused Science Topic Team should be that the work of the team will be greater than a simple sum of independent efforts of constituent members. At the same time, member PIs will have prepared proposals without knowing who will be selected for the team, so the opportunities for synergistic collaborations cannot be known a priori and cannot really be planned, or fully budgeted, at the proposal development stage. Individual PIs have a responsibility to complete the research they have proposed. Expectations for team participation, therefore, should not undermine individual project goals nor should they force participants to contribute an unfunded work effort in producing team deliverables.

With these caveats, and given the explicit guidelines for team participation in the TR&T Announcement of Opportunity, it is also expected that individual PIs will be prepared to devote reasonable effort in defining “a plan for structuring their work into an integrated research program” and in executing the plan to meet team goals.

If selected to serve as a team coordinator for focused science topic b) Effects of Ionospheric-Magnetospheric Plasma Redistribution on Storms, my responsibilities would include the following activities:

1. Schedule, coordinate and develop agendas for two team meetings per year, at least one to be held at NCAR/HAO, which has offered pro bono facility use for such meetings; a second annual meeting might be scheduled in conjunction with a regular professional meeting or conference;
2. Work with team members in developing a consensus on the scope of the team effort, including measures of success and deliverables for the integrated effort. Among various possibilities for deliverables I can envision:
 - a. special sessions devoted to the focused science topic at scientific meetings, with contributed and invited papers from team members and perhaps also from the larger research community;
 - b. collaborative efforts among team members to produce new models, tools, or scientific results that transcend individual efforts; such efforts would almost certainly have to be opportunistic, and where appropriate, they should be encouraged;
 - c. preparation of a special journal issue reporting scientific results of the team;
 - d. community challenges led by the team to engage the research community more broadly in its efforts, e.g., in comparing observations and model results – the GEM challenges may serve as a useful template for this mode; and
 - e. other concepts that are likely to emerge at team meetings;
3. Explore opportunities for inter-team synergies involving other focused science topics with overlapping interests; this activity might be initiated first at the team coordinator level;
4. Serve as lead liaison with the LWS Project Office at NASA’s Goddard Space Flight Center (GSFC) and LWS Program Office at NASA Headquarters, in monitoring and assisting the progress of the team. The mode of liaising would need to be negotiated with the program office; and
5. Lead the team effort in developing a final Team Report at the conclusion of the project. This report might take the form listed in 2c above with an appropriate introductory overview describing the nature, goals and success of the team project.

An effort would be made to schedule the first team meeting as soon as schedules permit after the selections are announced, but not later than August 31, 2007.

References

- Abe, T., A.W. Yau, S. Watanabe, and M. Yamada, E. Sagawa (2004), Long-term variation of the polar wind velocity and its implication for the ion acceleration process: Akebono/suprathermal ion mass spectrometer observations. *J. Geophys. Res.* *109*, A09305, doi:10.1029/2003JA010223.
- André, M., et al. (1998), Ion energization mechanisms at 1700 km in the auroral region, *J. Geophys. Res.* *103*, 4199.
- Banks, P.M. and T.E. Holzer (1968), The polar wind. *J. Geophys. Res.* *73*, 6846-6854.
- Bouhram, M., et al. (2004), On the altitude dependence of transversely heated O⁺ distributions in the cusp/cleft. *Ann. Geophys.* *22*, 1787-1798, doi:1432-0576/ag/2004-22-1787.
- Bouhram, M., et al. (2005), Survey of energetic O⁺ ions near the dayside mid-latitude magnetopause with Cluster. *Ann. Geophys.* *23*, 1281-1294.
- Cannata, R.W. and T.I. Gombosi (1989), Modeling the solar cycle dependence of quiet-time ion upwelling at geomagnetic latitudes. *Geophys. Res. Lett.* *16* (10), 1141-1144.
- Chappell, C.R., B.L. Giles, T.E. Moore, D.C. Delcourt, P.D. Craven, and M.O. Chandler (2000), The adequacy of the ionospheric source in supplying magnetospheric plasma. *J. Atmos. Sol.-Terr. Phys.* *62*, 421-436.
- Chaston, C.C., et al. (2004), Auroral ion acceleration in dispersive Alfvén waves. *J. Geophys. Res.* *109*, A04205, doi:10.1029/2003JA010053.
- Chaston, C.C., et al. (2005), Energy deposition by Alfvén waves into the dayside auroral oval: Cluster and FAST observations. *J. Geophys. Res.* *110*, A02211, doi:10.1029/2004JA010483.
- Cladis, J. B. (1986). Parallel acceleration and transport of ions from polar ionosphere to plasma sheet. *Geophys. Res. Lett.* *13*, 893.
- Craven, T.E., C.J. Lindgren, and S.A. Ledvina (1998), A two-dimensional multifluid MHD model of Titan's plasma environment, *Planet. Space Sci.* *46*, 1193-1205, 1998.
- Cully, C.M., E.F. Donovan, A.W. Yau, and G.G. Arkos (2003), Akebono/suprathermal mass spectrometer observations of low-energy ion outflow: Dependence on magnetic activity and solar wind conditions. *J. Geophys. Res.* *108* (A2), 1093, doi:10.1029/2001JA009200.
- Daglis, I. A. and W.I. Axford (1996), Fast ionospheric response to enhanced activity in geospace: Ion feeding of the inner magnetotail. *J. Geophys. Res.* *101*, 5047-5065.
- Daglis, I.A., et. al. (2003), Intense space storms: Critical issues and open disputes. *J. Geophys. Res.* *108* (A5), 1208, doi:10.1029/2002JA009722.
- Fedder, J.A., and J.G. Lyon (1987), The solar wind-magnetosphere-ionosphere current-voltage relationship. *Geophys. Res. Lett.* *14*, 880- 883.
- Fedder, J. A., S. P. Slinker, J. G. Lyon, and R. D. Elphinstone (1995), Global numerical simulation of the growth phase and expansion onset for a substorm observed by Viking, *J. Geophys. Res.*, *100*, 19,083.
- Foster, J.C., A.J. Coster, P.J. Erickson, F.J. Rich, B.R. Sandel (2004), Stormtime observations of the flux of plasmaspheric ions to the dayside cusp/magnetopause. *Geophys. Res. Lett.* *31*, L08809, doi:10.1029/2004GL020082.
- Foster, J.C., et al. (2005), Multiradar observations of the polar tongue of ionization. *J. Geophys. Res.* *110*, A09S31, doi:10.1029/2004JA010928.
- Gagne, J.R. (2005), *Implementation of Ionospheric Outflow in the LFM Global Magnetospheric Simulation*, M.S. Thesis, <http://engineering.dartmouth.edu/spacescience/wl/pub/Gagne05.pdf>, Dartmouth.
- Goldstein, J. and B.R. Sandel (2005), The global pattern of evolution of plasmaspheric drainage plumes, *Inner Magnetosphere Interactions: New Perspectives from Imaging*, AGU Geophysical Monograph 159, Proceedings of the 2004 Yosemite Workshop, (Burch, Schulz, Spence, eds.), 1-22, doi:10.1029/2004BK000104.
- Goodrich, C.C., A.L. Sussman, J.G. Lyon, M.A. Shay, and P.A. Cassak (2004), The CISM code coupling strategy, *J. Atmos. Sol.-Terr. Phys.* *66*, 1469, doi:10.1016/j.jastp.2004.04.010.
- Gorney, D. J., Y.T. Chiu, and D.R. Croley (1985), Trapping of ion conics by downward parallel electric fields. *J. Geophys. Res.* *90*, 4205.
- Grebowsky, J.M. (1970), Model study of plasmopause motion, *J. Geophys. Res.* *75*, 4329.
- Hain, K. (1987), The partial donor method, *J. Comp. Phys.* *73*, 131.

- Hairston, M.R., K.A. Drake and R. Skoug (2005), Saturation of the ionospheric polar cap potential during the October–November 2003 superstorms. *J. Geophys. Res.* *110*, A09S26, doi:10.1029/2004JA010864.
- Huddleston, M.M., C.R. Chappell, D.C. Delcourt, T.E. Moore, B.L. Giles, and M.O. Chandler (2005), An examination of the process and magnitude of ionospheric plasma supply to the magnetosphere. *J. Geophys. Res.* *110*, A12202, doi:1029/2004JA010401.
- Johnson, J.R. and C.Z. Cheng (2004), A self-consistent approach to modeling ion outflows associated with electromagnetic ion cyclotron waves, *EOS Trans. AGU*, *85*(17), Jt. Assem. Suppl., Abstract SM33A-15 (<http://w3.pppl.gov/~jrj/agu-icw-2004s.pdf>).
- Kelley, M.C., M.N. Vlasov, J.C. Foster, and A.J. Coster (2004), A quantitative explanation for the phenomenon known as storm-enhanced density. *Geophys. Res. Lett.* *31*, L19809, doi:10.1029/2004GL020875.
- Kistler, L.M., et al. (2005), Contribution of nonadiabatic ions to the cross-tail current in an O⁺ dominated thin current sheet. *J. Geophys. Res.* *110*, A06213, doi:10.1029/2004JA010653.
- Kulsrud, R.M., MHD description of plasma (1983), in *Handbook of Plasma Physics*, eds. M.N. Rosenbluth and R.Z. Sagdeev: Volume 1: Basic Plasma Physics, eds. A.A. Galeev and R.N. Sudan, 115-145, North-Holland Publishing Company, NY.
- Lemaire, J. F. and K. I. Gringauz (1998), *The Earth's Plasmasphere*. Cambridge: Cambridge University Press.
- Lennartsson, O.W., H.L. Collin, and W.K. Peterson (2004), Solar wind control of Earth's H⁺ and O⁺ outflow rates in the 15-eV to 33-keV energy range. *J. Geophys. Res.* *109*, A12212, doi:10.1029/2004JA010690.
- Lennartsson, O.W. and R.D. Sharp (1982), A comparison of the 0.1-17 keV/e ion composition in the near equatorial magnetosphere between quiet and disturbed conditions. *J. Geophys. Res.* *87* (A8), 6109-6120.
- Liemohn, M.W., et al. (2001), Dominant role of the asymmetric ring current in producing the stormtime Dst*. *J. Geophys. Res.* *106*, 10,883–10,904.
- Liu, C., J.L. Horwitz, and P.G. Richards (1995), Effects of frictional ion heating and soft-electron precipitation on high-latitude F-region upflows. *Geophys. Res. Lett.* *22*, 2713–2716.
- Liu, Y., A.F. Nagy, C.L. Groth, D.L. DeZeeuw, T.I. Gombosi, and K.G. Powell (1999), 3D multi-fluid MHD studies of the solar wind interaction with Mars, *Geophys. Res. Lett.* *26*, 2689-2692.
- Lockwood, M., M.O. Chandler, J.L. Horwitz, J.H. Waite, Jr., T.E. Moore, and C.R. Chappell (1985), The cleft ion fountain. *J. Geophys. Res.* *90*, 9736-9748.
- Lotko, W. (2004), Inductive magnetosphere-ionosphere coupling, *J. Atmos. Sol.-Terr. Phys.* *66*(15-16), 1443-1456.
- Lotko, W. (2006), The magnetosphere-ionosphere system from the perspective of plasma circulation, *J. Atmos. Sol.-Terr. Phys.*, accepted (<http://thayer.dartmouth.edu/spacescience/wl/pub/Lotko06.pdf>)
- Lund, E. J., et al. (2000), Transverse ion acceleration mechanism in the aurora at solar minimum: occurrence distributions. *J. Atmos. Sol.-Terr. Phys.* *62*, 467–475.
- Lynch, K.A., J.W. Bonnell, C.W. Carlson, and W.J. Peria (2002), Return current region aurora: E_{||}, j_z, particle energization, and broadband ELF wave activity. *J. Geophys. Res.* *107*(A7), 1115, 10.1029/2001JA900134.
- Lyon, J. G., J. A. Fedder, and C. M. Mobarry (2004), The Lyon-Fedder-Mobarry (LFM) global MHD magnetospheric simulation code, *J. Atmos. Sol.-Terr. Phys.* *66*(15-16), 1333-1350, 2004.
- Merkine, V.G., K. Papadopoulos, G. Milikh, A.S. Sharma, X. Shao, J. Lyon, and C. Goodrich (2003), Effects of the solar wind electric field and ionospheric conductance on the cross polar cap potential: Results of global MHD modeling. *Geophys. Res. Lett.* *30* (23), 2180, doi:10.1029/2003GL017903.
- Moore, T.E., et al. (1999), Ionospheric mass ejection in response to a CME. *Geophys. Res. Lett.* *26*, 2339.
- Nagy A.F., et al. (2001), The interaction between the magnetosphere of Saturn and Titan's ionosphere, *J. Geophys. Res.* *106*, 6151-6160.
- Nosé, M., S. Taguchi, K. Hosokawa, S.P. Christon, R.W. McEntire, T.E. Moore, M.R. Collier (2005), Overwhelming O⁺ contribution to the plasma sheet energy density during the October 2003 superstorm: Geotail/EPIC and IMAGE/LENA observations. *J. Geophys. Res.* *110*, A09S24, doi:10.1029/2004JA010930.

- Ober, D.M., N.C. Maynard, and W.J. Burke (2003), Testing the Hill model of transpolar potential saturation, *J. Geophys. Res.* 108(A12), 1467, doi:10.1029/2003JA010154.
- Olsson, A., P. Janhunen, T. Karlsson, N. Ivchenko, and L.G. Blomberg (2004), Statistics of Joule heating in the auroral zone and polar cap using Astrid-2 satellite Poynting flux. *Ann. Geophys.* 22, 4133-4142.
- Peterson, W.K., R.D. Sharp, E.G. Shelley, R.G. Johnson, and H. Balsinger (1981), Energetic ion composition of the plasma sheet. *J. Geophys. Res.* 86, 761.
- Peterson, W.K. (2002), Ionospheric influence on substorm development. In: Winglee, R.M. (Ed.), Proceedings of the 6th International Conference on Substorms (ICS-6). University of Washington, Seattle, pp. 143-150.
- Peterson, W.K., H.L. Collin, O.W. Lennartsson, and A.W. Yau (2006), Quiet time solar illumination effects on the fluxes and characteristic energies of ionospheric outflow. *J. Geophys. Res.*, in press.
- Robinson, R.M., R.R. Vondrak, K. Miller, T. Dabbs and D. Hardy (1987), On calculating ionospheric conductances from the flux and energy of precipitating electrons, *J. Geophys. Res.* 92, pp. 2565-2569.
- Roble, R.G., E.C. Ridley, A.D. Richmond and R.E. Dickinson (1988), A coupled thermosphere/ionosphere general circulation model, *Geophys. Res. Lett.* 15, 1525-2528.
- Russell, C.T., J.G. Luhmann, and G. Lu (2001), Nonlinear response of the polar ionosphere to large values of the interplanetary electric field. *J. Geophys. Res.* 106(A9), 18,495-18,504.
- Sato, T. (1959), Morphology of ionospheric F_2 disturbances in the polar regions: A linkage between polar patches and plasmaspheric drainage plumes. *Reports on Ionospheric Research and Space Research of Japan* 13, 91.
- Sauvaud, J.-A., et al. (2004), Case studies of the dynamics of ionospheric ions in the Earth's magnetotail. *J. Geophys. Res.* 109, A01212, doi:10.1029/2003JA009996.
- Schunk, R.W. and J.J. Sojka (1997), Global ionosphere-polar wind system during changing magnetic activity. *J. Geophys. Res.* 102, 11,625-11,651.
- Seki, K., M. Hirahara, T. Terasawa, T. Mukai, Y. Saito, S. Machida, Y. Yamamoto, S. Kokubun (1998), Statistical properties and possible supply mechanism of tailward cold O⁺ beams in the lobe/mantle regions. *J. Geophys. Res.* 103, 4477.
- Semeter, J., C.J. Heinselman, J.P. Thayer, and H.U. Frey (2003), Ion upflow enhanced by drifting F-region plasma structure along the nightside polar cap boundary. *Geophys. Res. Lett.* 30 (22), 2139, doi:10.1029/2003GL017747.
- Sharp, R.D., D.L. Carr, W.K. Peterson, and E.G. Shelley (1981), Ion streams in the magnetotail, *J. Geophys. Res.* 86 (A6), 4639-4648.
- Shay, M.A. and M. Swisdak (2004), Three-species collisionless reconnection: Effect of O⁺ on magnetotail reconnection. *Phys. Rev. Lett.* 93(17), 175001(4).
- Siscoe, G.L., J. Raeder, and A.J. Ridley (2004), Transpolar potential saturation models compared. *J. Geophys. Res.* 109, A09203, doi:10.1029/2003JA010318.
- Sojka, J.J., et al. (1993), Modeling polar cap F-region patches using time varying convection. *Geophys. Res. Lett.* 20, 1783.
- Sojka, J., R. Schunk, M. Bowline, J. Chen, S. Slinker, and J. Fedder (1997), Driving a physical ionospheric model with a magnetospheric MHD model, *J. Geophys. Res.*, 102, 22,209.
- Sojka, J.J., M.V. Subramaniam, L. Zhu, and R.W. Schunk (1998a), Gradient-drift instability growth rates from global scale modeling of the polar ionosphere. *Radio Sci.* 33 (6), 1915-1928.
- Sojka, J.J., R.W. Schunk, M.D. Bowline, J. Chen, S. Slinker, J. Fedder, P.J. Sultan (1998b), Ionospheric storm simulations driven by MHD and by empirical models with data comparisons, *J. Geophys. Res.* 103(A9), 20,669-20,684.
- Strangeway, R.J., R.E. Ergun, Y.-J. Su, C.W. Carlson, and R.C. Elphic (2005), Factors controlling ionospheric outflows as observed at intermediate altitudes. *J. Geophys. Res.* 110, A03221, doi:10.1029/2004JA010829.
- Tung, Y.-K., C.W. Carlson, J.P. McFadden, D.M. Klumpar, G.K. Parks, W.J. Peria, K. Liou (2001), Auroral polar cap boundary ion conic outflow observed on FAST. *J. Geophys. Res.* 106 (A3), 3603-3614.

- Wang, W., T.L. Killeen, A.G. Burns, et al. (1999), A high-resolution, three-dimensional, time dependent, nested grid model of the coupled thermosphere-ionosphere, *J. Atmos. Sol.-Terr. Phys.*, 61 (5), 385.
- Wang, W., T.L. Killeen, A.G. Burns and B.W. Reinisch (2001), A real-time model-observation comparison of F_2 electron densities during the Upper Atmospheric Research Collaboratory campaign of October 1997, *J. Geophys. Res.* 106, 21077–21082.
- Wang, W., M. Wiltberger, A.G. Burns, S. Solomon, T.L. Killeen, N. Maruyama, and J. G. Lyon (2004), Initial results from the coupled magnetosphere-ionosphere-thermosphere model: Thermosphere-ionosphere responses, *J. Atmos. Sol.-Terr. Phys.* 66(15-16), 1425-1441.
- Wang, W. A.G. Burns, S. Solomon, and T.L. Killeen (2005), High-resolution, coupled thermosphere-ionosphere models for space weather applications, *Adv. Space Res.* 36, 2486, doi:10.1016/j.asr.2003.11.025.
- Wiltberger, M., W. Wang, A. Burns, S. Solomon, J.G. Lyon, and C.C. Goodrich (2004), Initial results from the coupled magnetosphere- ionosphere-thermosphere model: Magnetospheric and ionospheric responses, *J. Atmos. Sol.-Terr. Phys.* 66(15-16), 1411-1423.
- Winglee, R. M., (1998a), Multi-fluid simulations of the magnetosphere: The identification of the geopause and its variation with IMF, *Geophys. Res. Lett.*, 25, 4441.
- Winglee, R. M., (1998b) Imaging the ionospheric and solar wind sources in the magnetosphere through multi-fluid global simulations, *Phys. Space Plasmas*, 15, 345.
- Winglee, R.M., Chua, D., Brittnacher, M., Parks, G.K., and Lu, G. (2002), Global impact of ionospheric outflows on the dynamics of the magnetosphere and cross-polar cap potential. *J. Geophys. Res.* 107 (A9), 1237, doi:10.1029/2001JA000214.
- Winglee, R.M. (2004), Ion cyclotron and heavy ion effects on reconnection in a global magnetotail, *J. Geophys. Res.* 109, A09206, doi:10.1029/2004JA010385.
- Yau, A.W. and M. André (1997), Source of ion outflow in the high latitude ionosphere, *Space Sci. Rev.* 80, 1.
- Zheng, Y., T.E. Moore, F.S. Mozer, C.T. Russell, and R.J. Strangeway (2005), Polar study of ionospheric ion outflow versus energy input. *J. Geophys. Res.* 110, A07210, doi:10.1029/2004JA010995.